USAARL-TECH-SR--2024-12

UNITED STATES ARMY AEROMEDICAL RESEARCH LABORATORY

Instrumented Mouthguard Laboratory Evaluation Using Two Anthropometric Test Device Headforms

Brandon A. Brown, Ray W. Daniel, & Tyler F. Rooks

Human Subjects Use

In the conduct of research involving human subjects, the investigator(s) adhered to the policies regarding the protection of human subjects as prescribed by Department of Defense Instruction 3216.02 (Protection of Human Subjects and Adherence to Ethical Standards in DoD-Supported Research) dated 8 November 2011.

REPORT DOCUMENTATION PAGE

Form Approved
OMB No. 0704-0188

1. REPORT DATE *(DD-MM-YYYY)*: 12-12-2024

2. REPORT TYPE: Special Report

3. DATES COVERED *(From - To)*: 15 JAN 2017 - 21 OCT 2021

4. TITLE AND SUBTITLE
Instrumented Mouthguard Laboratory Evaluation using Two Anthropometric Test Device Headforms

5a. CONTRACT NUMBER: W81XWH-17-1-0019

5b. GRANT NUMBER

5c. PROGRAM ELEMENT NUMBER

5d. PROJECT NUMBER: MOMRP 17220 (ESiT)

5e. TASK NUMBER

5f. WORK UNIT NUMBER

6. AUTHOR(S)
Brown, B. A.[1,2], Daniel, R. W.[1,2], & Rooks, T. F.[1]

7. PERFORMING ORGANIZATION NAME(S) AND ADDRESS(ES)
U.S. Army Aeromedical Research Laboratory
P.O. Box 620577
Fort Novosel, AL 36362

8. PERFORMING ORGANIZATION REPORT NUMBER: USAARL-TECH-SR--2024-12

9. SPONSORING/MONITORING AGENCY NAME(S) AND ADDRESS(ES)
U.S. Army Medical Research and Development Command
Military Operational Medicine Research Program
810 Schreider Street
Fort Detrick, MD 21702

10. SPONSOR/MONITOR'S ACRONYM(S): USAMRDC MOMRP

11. SPONSOR/MONITOR'S REPORT NUMBER(S)

12. DISTRIBUTION/AVAILABILITY STATEMENT
DISTRIBUTION STATEMENT A. Approved for public release; distribution is unlimited.

13. SUPPLEMENTARY NOTES
[1]U.S. Army Aeromedical Research Laboratory; [2]Katmai Government Solutions, LLC

14. ABSTRACT
This study is in support of the Human Head Impact Dose Concussion Risk Functions and Sensor-Based Military-Specific Environmental Monitoring System project (BA150149, W81XWH-17-1-0019). Test methods and results comparing the measured kinematics using a boil-and-bite instrumented mouthguard with reference kinematics from two ATD headforms under multiple exposure types and severities are provided. Mouthguard performance was comparable to prior literature; however, there was an increase in variability due to fitting. The Mandible Load Sensing Headform resulted in poor comparisons between the mouthguard and the reference due to several issues with jaw movement and interactions with the mouthguard. A modified NOCSAE headform resulted in good comparisons between the mouthguard and reference data. Increased variability in mouthguard response compared to the reference was primarily attributed to the use of boil-and-bite versus fully custom-molded mouthguards commonly used in the literature. While increased, when compared to custom-molded mouthguards, the variability was still minimal.

15. SUBJECT TERMS
environmental sensor, concussion, traumatic brain injury, TBI, mTBI, wearable sensor, concussion monitor, head impact sensor, ESiT

16. SECURITY CLASSIFICATION OF: a. REPORT	b. ABSTRACT	c. THIS PAGE	17. LIMITATION OF ABSTRACT	18. NUMBER OF PAGES	19a. NAME OF RESPONSIBLE PERSON
UNCLAS	UNCLAS	UNCLAS	SAR	22	Loraine St. Onge, PhD

19b. TELEPHONE NUMBER *(Include area code)*: 334-255-6906

This page is intentionally blank.

Table of Contents

Page

List of Figures

Table of Contents (continued)

Page

List of Tables

Background

The following report was provided to Dr. Adam Bartsch in support of the Human Head Impact Dose Concussion Risk Functions and Sensor-Based Military-Specific Environmental Monitoring System Project (BA150149, W81XWH-17-1-0019). Dr. Bartsch was the project Principal Investigator, and the U.S. Army Aeromedical Research Laboratory (USAARL) was a collaborator performing laboratory evaluations of the instrumented mouthguard from Prevent Biometrics using multiple anthropometric test devices (ATDs) (Bartsch, 2022). Assessments were completed in accordance with approved USAARL Test Plan 2020-016.

The information enclosed consists of test methods, instrumentation details, and results comparing the measured kinematics using a boil-and-bite instrumented mouthguard with reference kinematics from two ATD headforms under multiple exposure types and severities.

Introduction

Mild traumatic brain injury (mTBI) is a concern in military environments (Defense and Veterans Brain Injury Center [DVBIC], 2020). Immediate symptoms associated with mTBI (concussion) include loss of consciousness for up to 30 minutes, alteration of consciousness or mental state for up to 24 hours, and post-traumatic amnesia for up to 24 hours (O'Neil et al., 2013). Repeated mTBI is associated with longer recovery times and reduced ability to process information (Gronwall & Wrightson, 1975). Multiple mTBIs could potentially increase the risk of neurodegenerative disorders (McAllister & McCrea, 2017); while no link has definitively been established between Alzheimer's disease and repetitive mTBI, earlier onset of Alzheimer's was observed in a study of retired football players versus the general population (Guskiewicz et al., 2005).

Timely and accurate information is important for clinical diagnosis and return-to-duty following a concussion (Asken et al., 2016). Diagnoses often depend on self-reporting, which may result in missed diagnoses since individuals who suffer a concussion may not have awareness of symptoms (McCrea et al., 2004). Environmental sensors (ES) attached to a Soldier's helmet or head are a tool that may provide the ability to identify possible concussions in real time without relying on self-reporting. Environmental sensors record head accelerative exposures and give estimates of kinematics at the head center of gravity (CG). The Impact Monitor Mouthguard (IMM) developed by Prevent Biometrics (Edina, MN) is a mouthguard-based ES that could be used to measure kinematics at the head CG resulting from exposure. The IMM is capable of recording head kinematics (i.e., linear acceleration, angular velocity) associated with potentially concussive events (Bartsch et al., 2014; Bartsch et al., 2020; Liu et al., 2020; Jones et al., 2022; Kieffer et al., 2020).

For ESs to be useful, they need to give reasonable estimates of accelerative exposures at the head CG. Laboratory testing using ATDs is one way that mouthguard sensors have been validated (Bartsch et al., 2014; Camarillo et al., 2013; Kieffer et al., 2020; Kuo et al., 2016; Siegmund et al., 2016). Testing has generally included direct impacts to helmeted and un-helmeted ATDs of a 50th percentile male at increasing levels of severity (Bartsch et al., 2014; Camarillo et al., 2013; Kieffer et al., 2020; Kuo et al., 2016; Siegmund et al., 2016). Agreement levels between mouthguards and laboratory-grade sensors have ranged from excellent (Bartsch et al., 2014; Camarillo et al., 2013) to poor (Siegmund et al., 2016). Kuo et al. (2016) proved in a laboratory setting that one of the main factors in determining levels of agreement has been whether the ATD used in testing contains a clenched mandible, unconstrained mandible, or no mandible. These three mandible conditions were tested and used to reproduce data from previous studies (Bartsch et al., 2014; Camarillo et al., 2013; Siegmund et al., 2016). One factor not tested by these studies is the accuracy of the mouthguard sensors under indirect or inertial loading.

The objective of this study was to compare the kinematic response predicted by the instrumented mouthguard with that reported by a laboratory reference measured at the center of gravity of an ATD headform. Additionally, this study evaluated the influence of the choice of ATD headform (with varying mandible designs) and indirect (e.g., inertial) versus direct (e.g., impact) loadings.

Methods

The study was conducted at USAARL to determine the agreement between the IMM and laboratory-grade sensors at the head CG of multiple ATD headforms. Testing was conducted under direct and inertial loading. The IMM was tested during frontal impacts using a pendulum and minisled setup to determine how well it reproduces kinematics measured at the head CG via laboratory-grade sensors of a modified National Operating Committee on Standards for Athletic Equipment (NOCSAE) headform and a Mandible Load Sensing Headform (MLSH). The modified NOCSAE headform incorporated a screw through the bottom of the jaw to replicate conditions of a “clenched mandible,” and the MLSH was designed with a mandible that freely rotates and uses springs to simulate clamping forces in the jaw. Boxing headgear was also added to the ATD headforms for direct impacts to determine whether the headgear affects the accuracy of the IMM.

Minisled Test Device

The USAARL pendulum and minisled setup consists of a horizontal rail system (3.66 meters) and a low-friction sled. The sled is placed at one end of the track, and a 22.7 kilogram (kg) rigid direct impact pendulum (Figure 1) strikes the headform directly, simulating a boxer’s punch. The system can also be set up for indirect impacts via a 45.4 kg indirect impact pendulum, which simulates an inertial load to the sled representing the C7-T1 junction. Palmyra brushes bring the sled to a stop approximately 1.3 meters from the impact site. The pendulum release height can be adjusted to impact the system with varying amounts of intensity and energy.

This space is intentionally blank.

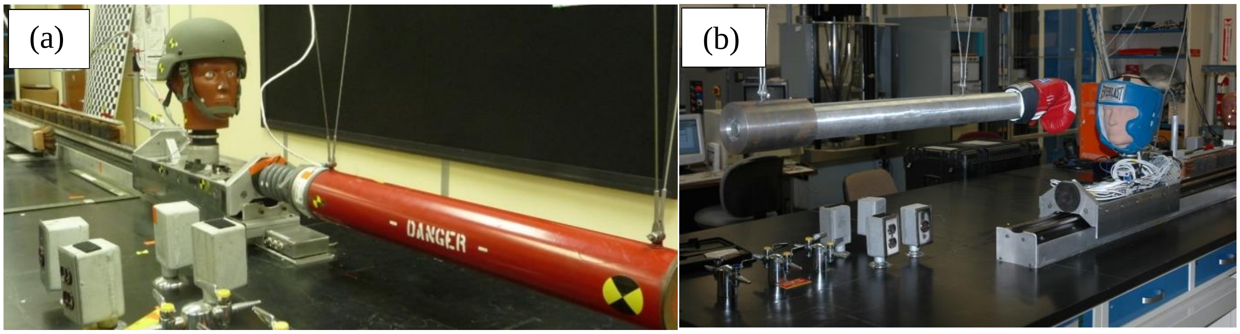

Figure 1. USAARL minisled system showing the (a) indirect or inertial loading setup and the (b) direct loading setup.

Anthropometric Test Device Headforms

The MLSH (Figure 2) is a 50th percentile Hybrid-III (H-III) ATD altered to have an articulating jaw that allows testing of a mouthguard sensor. The jaw contains a steel mandible with upper and lower simulated dentition and spring-loaded temporomandibular joints (TMJs). The TMJ produces a clamp/bite force of approximately 22.3 Newtons (N) (Siegmund et al., 2014). The headform connects to an H-III neck.

The NOCSAE headform (Figure 3) was designed for use in NOCSAE standards testing. The NOCSAE headform used in this study was altered to allow fitting of the IMM; an adapter was added to allow connection to an H-III neck. A slot in the face of the modified NOCSAE headform allows insertion of the IMM into the headform; a screw underneath the jaw allows simulation of a biting force by holding in place an aluminum plate underneath the IMM.

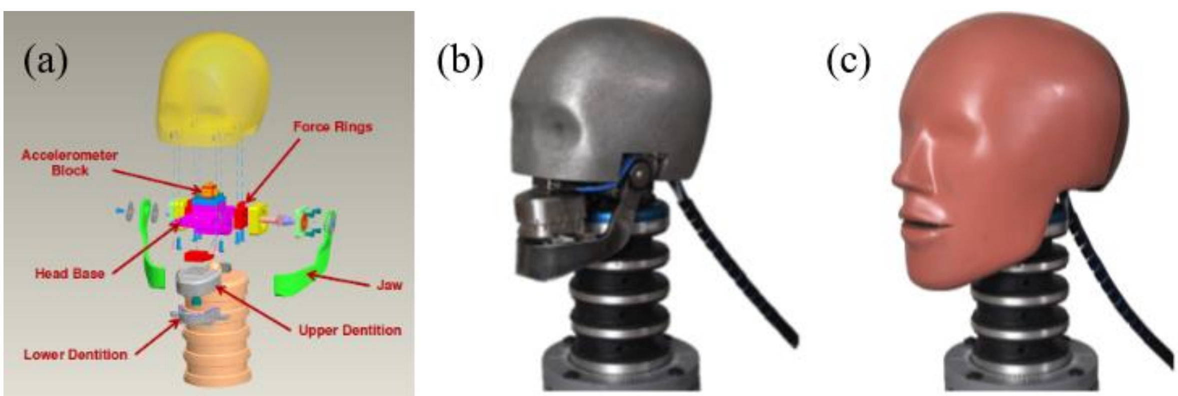

Figure 2. MLSH. (a) Exploded view, (b) assembled and attached to an H-III neck, and (c) with synthetic H-III skin.

This space is intentionally blank.

Figure 3. Modified NOCSAE headform with slot for the IMM and metal plate to hold the sensor onto the upper dentition.

Instrumentation

The MLSH was instrumented with a nine-accelerometer array (Endevco 7264B-2000) located at the head CG to transform linear acceleration into angular rate and angular acceleration during post-processing (Martin et al., 1998). The MLSH also included a six-degree-of-freedom (6-DOF) load cell (triaxial forces and triaxial moments) at the lower neck (Humanetics 7992JS1TF), 3-DOF load cells at the left and right TMJs (PCB Piezotronics 260A01), and a 3-DOF load cell at the upper dentition (PCB Piezotronics 260A01).

The NOCSAE headform was instrumented with three linear accelerometers (Endevco 7264C-2KTZ) and three angular rate sensors (DTS ARS PRO-8K) at the head CG. The NOCSAE headform had the same lower neck load cell as the MLSH but did not include TMJs or upper dentition load cells.

All tests included a uniaxial linear accelerometer on the sled carriage (Endevco 7264C-500). For indirect impacts, a triaxial force load cell was installed on the pendulum impactor (Humanetics 8728TF). For direct impacts, a uniaxial linear accelerometer (7264C-500TZ) was installed on the pendulum to measure linear acceleration. The linear accelerometer on the sled was used to determine the repeatability of the tests.

All laboratory-grade data was collected using the Synergy data acquisition system (High-Techniques, Madison, WI, USA) and sampled at 20,000 samples per second (sps). Additionally, high-speed video was captured for all tests at 1500 frames per second (fps) using a Vision Research Phantom Miro camera (Wayne, NJ, USA). Markers were placed on the headform, neck, and sled to track movement.

Test Conditions

Tests were conducted under both inertial (indirect) loading as well as direct loading using both the modified NOCSAE headform and MLSH. All tests were conducted with exposures in the -x direction (the direction of motion is opposite the direction the ATD was facing). For inertial loading, tests were conducted at four impact energies of approximately 130 Joules (J), 198 J, 266 J, and 334 J. For each energy, three different IMM sensors were tested. Impacts for a given energy and headform were repeated three times (Table A1).

For the direct impacts, tests were conducted at two different impact energies simulating the punch of a flyweight and super heavyweight boxer (Table A2; Tables B1 and B2) (Walilko et al., 2005). For each energy, three different IMM sensors were tested. Impacts for a given energy and headform were repeated three times with and without boxing headgear (Appendix A).

The Prevent Biometrics Impact Monitor Mouthguard (IMM)

The IMM is a hybrid boil-and-bite mouthguard with embedded flexible circuitry; a tri-axial gyroscope and three linear accelerometers are attached to the circuitry inside the mouthguard. The linear accelerometers and tri-axial gyroscope allow kinematics (i.e., head angular velocity/angular acceleration and linear acceleration) to be recorded at the mouth (Bartsch et al., 2014). Linear acceleration at the mouth is transformed to the head CG using rigid body kinematics via the following equation:

$$\vec{a}_{Head\_CG} = \vec{a}_{IMM} + \vec{\alpha}_{IMM} \times \vec{r}_{Head\_CG/IMM} + \vec{\omega}_{IMM} \times \left(\vec{\omega}_{IMM} \times \vec{r}_{Head\_CG/IMM}\right) \quad \text{(Equation 1)}$$

Where $\vec{a}_{Head\_CG}$ and $\vec{a}_{IMM}$ are linear accelerations at the head CG and mouthguard, respectively, and $\vec{r}_{Head\_CG/IMM}$ is the head CG position relative to the mouthguard. Finally, $\vec{\omega}_{IMM}$ and $\vec{\alpha}_{IMM}$ are the measured angular velocity and angular acceleration, respectively.

Before conducting the tests, the IMM was boiled for 50 seconds. The IMM was then held onto a jig for the MLSH tests and onto the headform dentition for the NOCSAE tests. The IMM was fit to each ATD for 30 seconds. After fitting, the IMM was placed onto each headform prior to testing. Data recorded by the headform was wirelessly transmitted to a computer for post-processing during testing. To confirm adequate coupling to the dentition, each IMM was placed on the dentition prior to testing, and it was confirmed that it stayed in place without additional clamping.

The IMM was set in “lab mode” for all tests. The trigger threshold was 5 G along any axis, and the internal filtering algorithms and requirements were disabled for the study to ensure data collection on the headforms. Upon passing the trigger threshold, the mouthguard provided linear acceleration, angular acceleration, and angular velocity time traces for each axis, as well as resultants at the head CG. Sampling rate for all data was 3200 hertz (Hz). Accelerometer and gyroscope ranges were +/- 200 G and +/- 2000 degrees per second (deg/s), respectively. The time of recorded data was 50 milliseconds (ms) with a 10 ms pre-trigger duration.

Table 1. The Prevent Biometrics Impact Monitor Mouthguard (IMM)

Sensor	**Mount type/location**	**Primary measurements, battery life, and trigger threshold**	
Prevent Biometrics IMM	Head/mouth (mouthguard)	Processed linear acceleration, angular velocity, and angular acceleration along/about *X*, *Y*, and *Z* axes at head CG in the J211 coordinate system Summary linear acceleration, angular acceleration, and angular velocity at head CG Sampling rate: 3200 Hz (all data) Battery life: ~10 hours (depends on activity level and wear of the device) Trigger: 5 G in any single axis Linear accelerometer range: +/- 200 G along each axis Gyroscope range: +/- 2000 deg/second about each axis Linear/angular acceleration and angular velocity duration and pre-trigger duration: 50 ms, 10 ms	 Source: https://preventbiometrics.com/the-system/

Data Analysis

All linear accelerometer and angular acceleration data at the head CG was filtered at a 200 Hz cutoff frequency during post-processing. Sled accelerometer, pendulum force, and pendulum accelerometer data were filtered at channel frequency class 60 (CFC 60) as defined in Society of Automotive Engineers (SAE) J211 standards (SAE, 1995). The coordinate system at the head CG followed SAE J211 with +x out the front of the face, +y out the right side of the head, and +z out the bottom of the head as defined by the right-hand rule (Figure 4). The internal coordinate system for the IMM was the same as the laboratory reference.

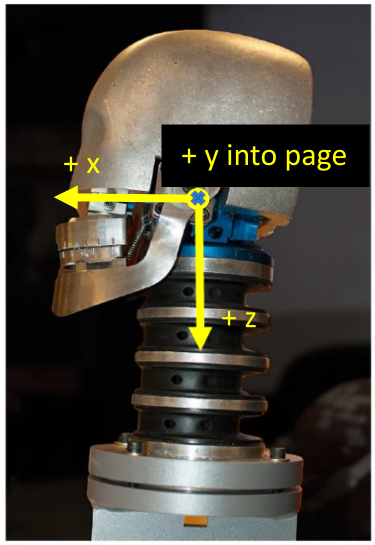

Figure 4. Head CG coordinate system of MLSH without synthetic skin. The coordinate system of the NOCSAE headform is the same as the MLSH.

Percent error between the laboratory (e.g., reference) instrumentation and the IMM was calculated to compare measurements from the IMM and kinematics at the head CG. Percent error is given by the following:

$$\text{Percent Error} = \frac{|Kinematic_{IMM} - Kinematic_{Reference}|}{Kinematic_{Reference}} * 100 \qquad \text{(Equation 2)}$$

Where $Kinematic_{IMM}$ and $Kinematic_{Reference}$ are the kinematic quantity being compared between the IMM and laboratory grade sensors, respectively. Kinematics compared between the IMM and laboratory reference instrumentation included peak resultant linear acceleration (PRLA) at the head CG and peak absolute value of pitch rate (PPR). Summary statistics of percent error between the IMM and reference were calculated for all tests. In addition, summary statistics were calculated for each of the test conditions (e.g., direct versus indirect exposure condition). Lines of best fit between the IMM and reference peak kinematic data were constructed across all tests for each combination of loading condition and ATD headform to determine how well IMM kinematics linearly correlated with ATD kinematics.

Results

For the resultant linear acceleration, indirect impact tests with the NOCSAE headform (7.46 ± 3.12%) had smaller mean percent error (MPE) than tests with the MLSH (21.2 ± 22.9%) (Figure 5). For the angular rate, indirect impact tests with the NOCSAE headform (3.80 ± 3.35%) also had smaller MPE than tests with the MLSH (9.72 ± 8.51%) (Figure 5).

For the resultant acceleration, direct impact tests with the NOCSAE headform (10.6 ± 9.03%) had smaller MPE than tests with the MLSH (27.6 ± 22.0%). For the angular rate, direct impact tests with the NOCSAE (1.22 ± 1.29%) also had smaller MPE than tests with the MLSH (14.1 ± 10.4%) (Figure 6).

The IMM had a nearly linear response compared with the NOCSAE headform for PRLA (slope: 1.04, R^2: 0.96) and PPR (slope: 0.96, R^2: 0.98) values across all indirect impacts (see corresponding lines of best fit in Figure 7 and Figure 8). Additionally, the IMM had a nearly linear response compared with the MLSH for PPR (slope: 1.1, R^2: 0.90) values across all indirect impacts (see corresponding line of best fit in Figure 8). PRLA values from the IMM did not have a linear response compared with the MLSH PRLA values (slope: 1.23, R^2: 0.68; Figure 7).

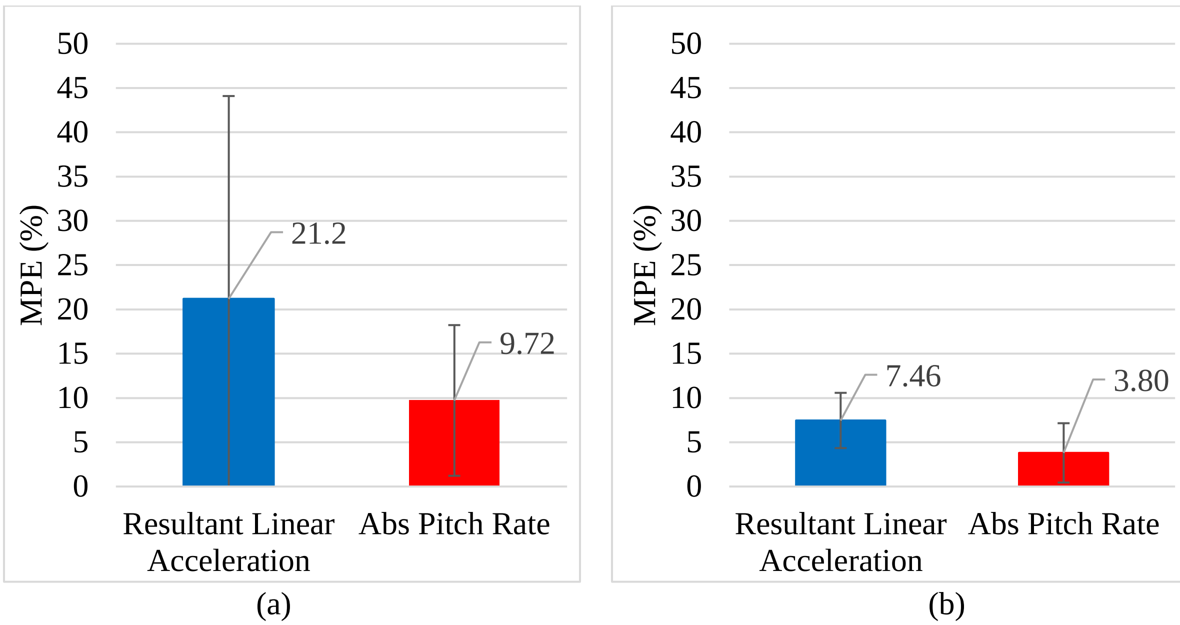

Figure 5. MPE between ATD and instrumented mouthguard peak kinematics for (a) the MLSH and (b) the NOCSAE headform during indirect impacts. For both ATDs, the MPE for the angular rate was consistently lower than the resultant linear acceleration. "Abs Pitch Rate" is the absolute value of the pitch rate.

This space is intentionally blank.

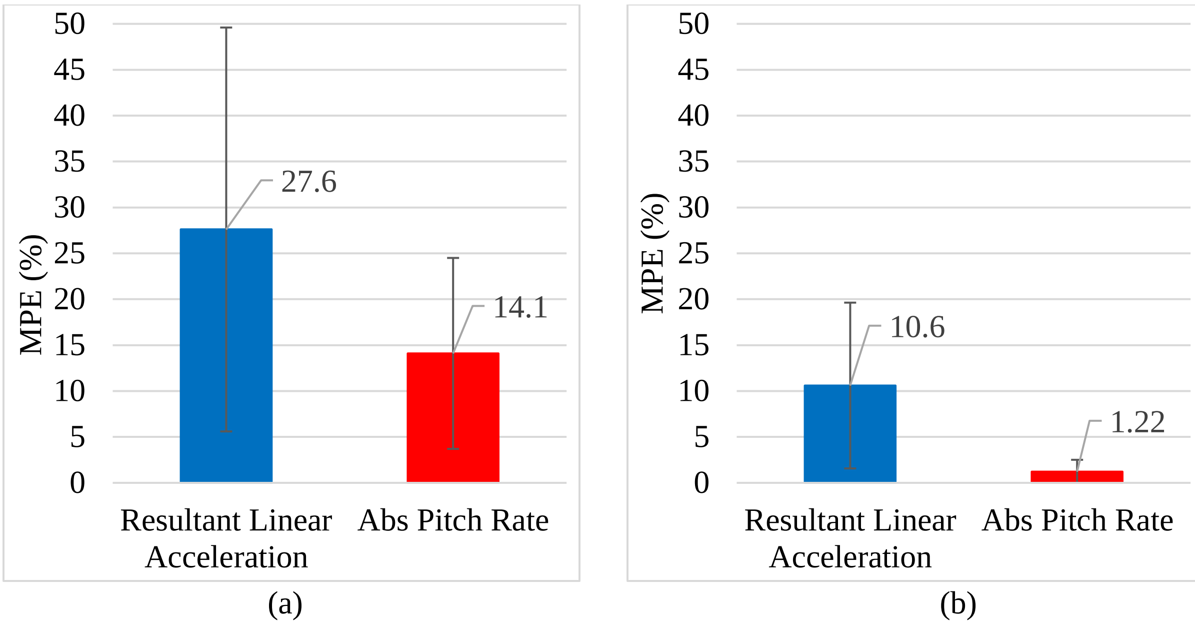

Figure 6. Mean percent error between ATD and instrumented mouthguard peak kinematics for (a) the MLSH and (b) the NOCSAE headform during direct impacts. For both ATDs, the MPE for the angular rate was consistently lower than the resultant linear acceleration. "Abs Pitch Rate" is the absolute value of the pitch rate.

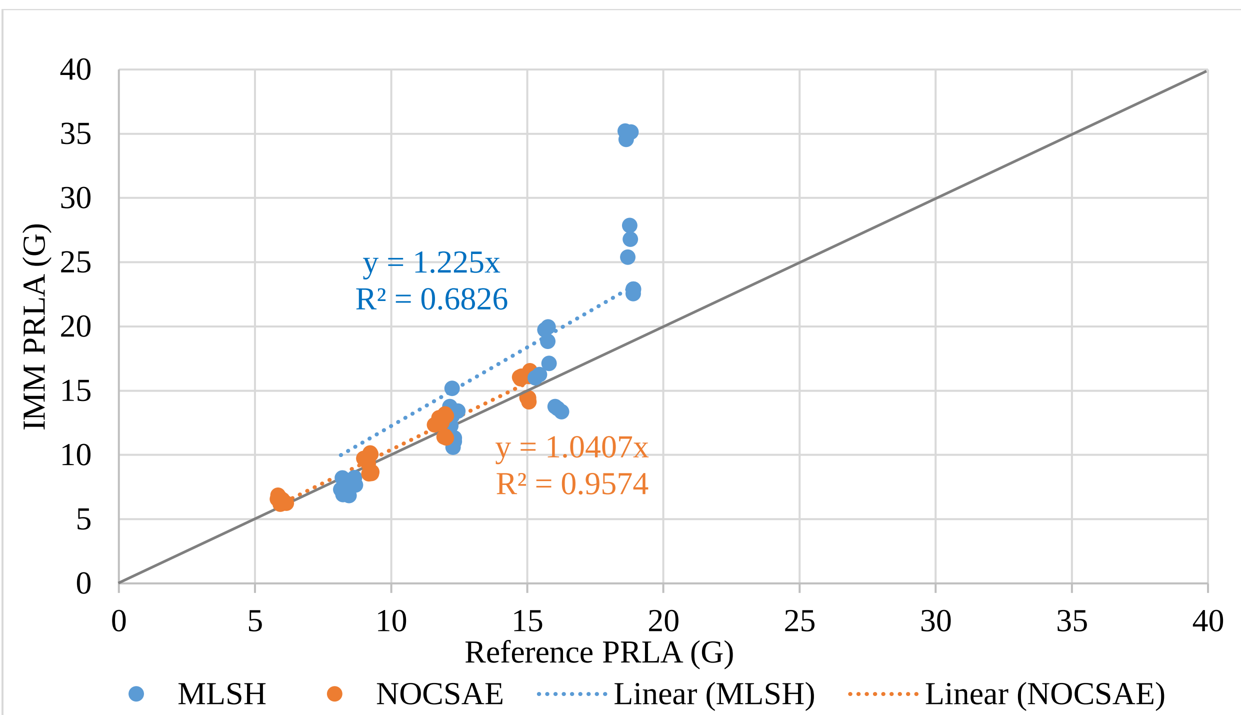

Figure 7. Scatter plot of ATD and instrumented mouthguard peak linear acceleration during indirect impacts. The NOCSAE headform had good agreement throughout the test range while the MLSH headform had large errors at the higher test energies.

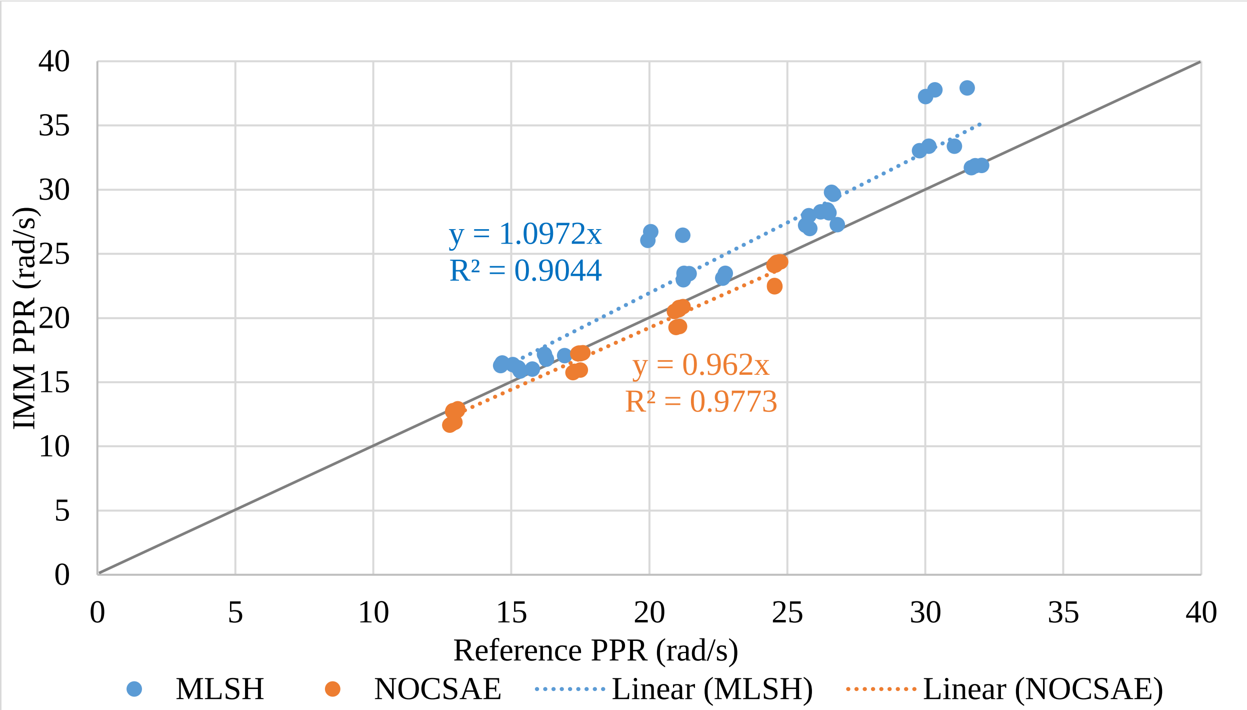

Figure 8. Scatter plot of ATD and instrumented mouthguard peak angular velocity during indirect impacts. For PPR, the instrumented mouthguard response agreed well with both ATDs. *Angular velocity is reported in radians per second (rad/s).

The IMM showed a nearly linear response compared with the NOCSAE headform for PRLA (slope: 0.99, R^2: 0.82) and PPR (slope: 1.01, R^2: 0.99) values across all direct impacts (see corresponding lines of best fit in Figure 9 and Figure 10). The IMM had a nearly linear response compared with the MLSH PPR (slope: 1.14, R^2: 0.83) values across all direct impacts (see corresponding line of best fit in Figure 10). While PRLA response from the IMM was nearly linear compared with the MLSH PRLA values (slope: 1.33, R^2: 0.88; Figure 9), there was a substantial increase in the error of IMM responses at higher energies compared to the MLSH PRLA.

This space is intentionally blank.

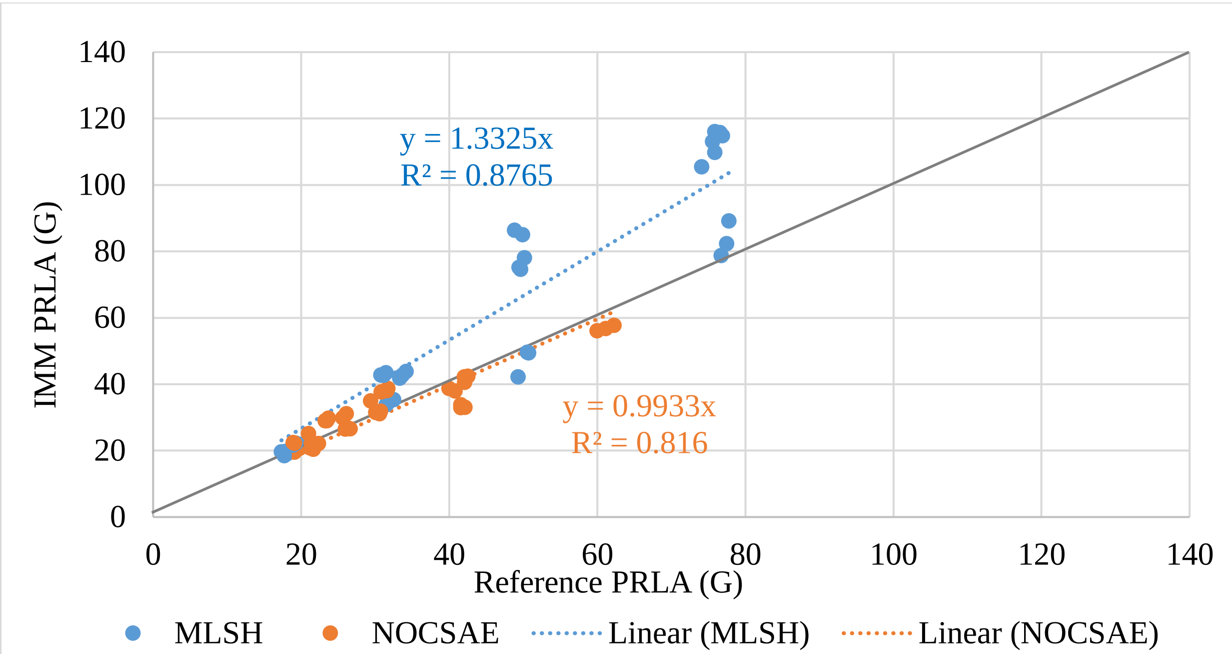

Figure 9. Scatter plot of ATD and instrumented mouthguard peak linear acceleration during direct impacts. The NOCSAE headform had good agreement throughout the test range while the MLSH headform had large errors at the higher test energies.

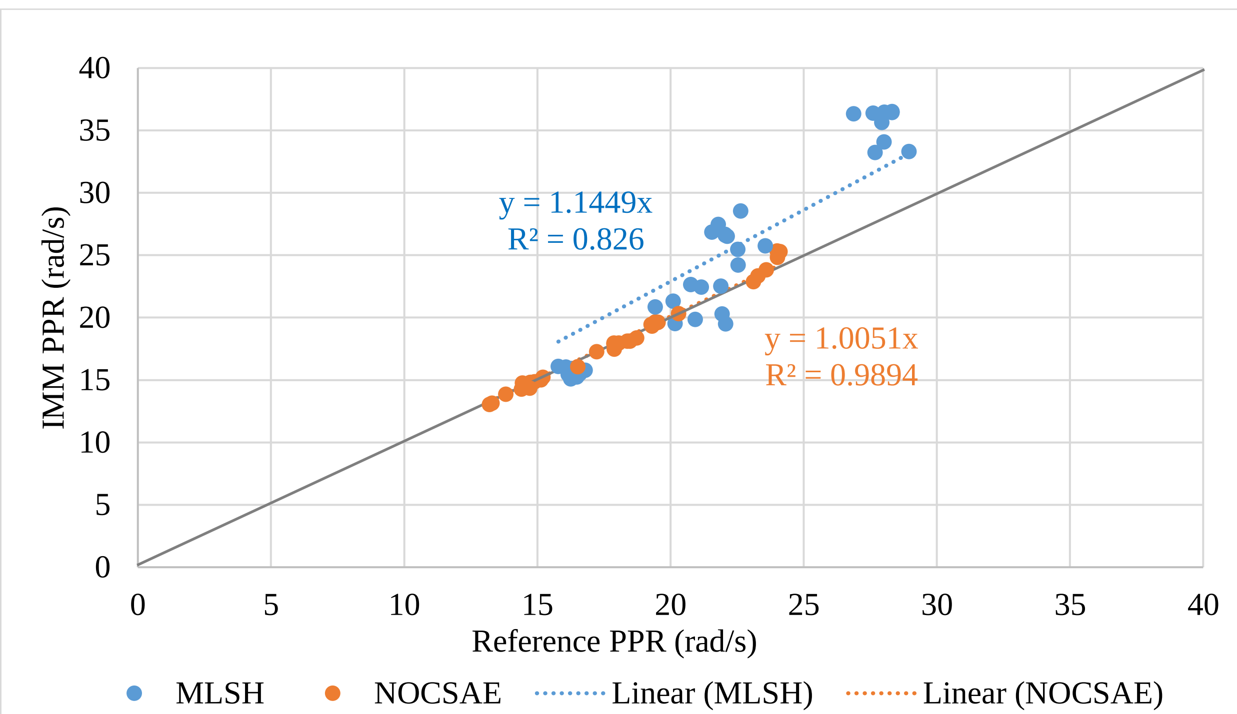

Figure 10. Scatter plot of ATD and instrumented mouthguard peak angular velocity during direct impacts. For PPR, the instrumented mouthguard response agreed well with both ATDs; however, MLSH tests had a slight overestimation.

Discussion

In general, the agreement between IMM and ATD kinematic data was better for the NOCSAE headform than for the MLSH (Figures 5-10). This finding is in agreement with previous literature (Camarillo et al., 2013; Siegmund et al., 2014; Kuo et al., 2016; Liu et al., 2020; Kieffer et al., 2020; Jones et al., 2022). The NOCSAE headform contains what is known as a "clenched" mandible in previous literature, while the MLSH mandible is not fully constrained and can rotate freely as the headform rotates. Kuo et al. (2016) evaluated a mouthguard formed using ATD dentition molds under direct impacts for three mandible conditions, including no mandible, clenched mandible, and unconstrained mandible. Linear regression analyses between ATD and mouthguard peak resultant linear acceleration and peak resultant angular velocity across all impacts resulted in slopes of 0.99 and 1.01, respectively. For the clenched mandible condition, this finding is similar to what has been shown in the current study (Figures 7-10). Similar to the MLSH results for the present study, Kuo et al. (2016) stated that for the unconstrained mandible condition, mouthguard peak resultant angular velocity and peak resultant linear acceleration generally over-predicted corresponding reference measurements. Further, Camarillo et al. (2013) and Kieffer et al. (2020) discuss similar findings to the present study using a clenched mandible under direct impacts (excellent agreement between sensor and ATD kinematic measurements). Finally, Siegmund et al. (2014) reported absolute errors of 12 ± 10% across multiple impact sites and severities when testing a mouthguard under direct impacts using the MLSH.

MPE between NOCSAE headform and IMM PRLA and PPR had smaller percentages and standard deviations than that of the MLSH (Figures 5 and 6). The NOCSAE headform also had better linear correlation with IMM PRLA than that of the MLSH for both indirect and direct impacts (Figures 7-10). The linearity between the IMM and ATD highlighted the effects of the unconstrained mandible in the MLSH through increased slope compared to the expected value as well as the lower R^2 values.

The R^2 values in the present study were lower than in prior work. In comparison with prior work evaluating instrumented mouthguards, the present study did not use custom-molded mouthguards but instead used boil-and-bite versions that were manually fit to the ATD. The lower R^2 values were determined to be due to mouthguard fit. When reviewing individual IMM responses compared with the ATDs, substantial differences in slope and R^2 were observed for some of the IMMs, indicating differences in fit (Appendix C). As with the data considered across sensor groups, the IMM and NOCSAE headform kinematics were more similar than the MLSH and IMM kinematics. When reviewing data broken down by sensor group, it was determined that one of the sensor groups was uniquely non-correlated with the corresponding NOCSAE headform PRLA values during direct impacts (Appendix C). This finding likely contributed to the lower R^2 values when considered across sensor groups. Issues fitting the mouthguard could cause sensors to be oriented incorrectly or cause the mouthguard to slip on the teeth. Previous work has shown that the orientation of a sensor affects agreement with measurements at the head CG (Brown et al., 2021). These findings highlight the potential variability in mouthguard response due to poor fit. Further, the findings stress the importance of ensuring a good fit both during laboratory testing and during field studies.

There were limitations in this study. First, only one impact direction was considered. Agreement between ATD and mouthguard data has been shown to be location-dependent, and our results could be different if considering other directions. One takeaway of the study, that a clenched ATD mandible gives better agreement with IMM kinematics than a freely rotating ATD mandible, has been shown in previous literature to be true across several impact locations (Siegmund et al., 2014; Kuo et al., 2016). It is anticipated that this study would show the same findings if more impact locations were tested. Second, this study used one size for both the MLSH and NOCSAE headforms. Headforms of different sizes may affect the ability of IMM internal algorithms to predict kinematics at the head CG accurately.

Agreement between the IMM and ATD kinematics was found to be dependent on the headform used as well as the mouthguard fit. These results are not unexpected based on previously summarized literature and their agreement with the results of this study. A freely rotating mandible will strike the IMM, causing motion independent of the primary motion of the head. This will result in independent movement of the IMM accelerometers and tri-axial gyroscope, leading to inaccurate measurements. While the variability in response increased for the boil-and-bite IMM used in this study, the overall variability remained small. Compared with prior literature that used custom-molded mouthguards during laboratory evaluations, the variability in fit due to boil-and-bite procedures provides a more representative sample of the currently used devices in human subject research applications and of the potential variation in fit for human subjects. This suggests that boil-and-bite mouthguards could be used for research with minimal increases in potential errors estimating head acceleration exposures.

References

Asken, B. M., McCrea, M. A., Clugston, J. R., Snyder, A. R., Houck, Z. M., & Bauer, R. M. (2016). Playing through it: Delayed reporting and removal from athletic activity after concussion predicts prolonged recovery. *Journal of Athletic Training*, *51*(4), 329–335. https://doi.org/10.4085/1062-6050-51.5.02

Bartsch, A. (2022). *Human head impact dose concussion risk functions and sensor-based military-specific environmental monitoring system* (Final Contract Report W81XWH-17-1-0019). Prevent Biometrics.

Bartsch, A., Samorezov, S., Benzel, E., Miele, V., & Brett, D. (2014). *Validation of an "intelligent mouthguard" single event head impact dosimeter* (Technical Paper No. 2014-22-0001). SAE. https://doi.org/10.4271/2014-22-0001

Bartsch, A. J., Hedin, D., Alberts, J., Benzel, E. C., Cruickshank, J., Gray, R. S., Cameron, K., Houston, M. N., Rooks, T. F., McGinty, G., Kozlowski, E., Rowson, S., Maroon, J. C., Miele, V. J., Ashton, J. C., Siegmund, G. P., Shah, A., McCrea, M., & Stemper, B. (2020). High energy side and rear American football head impacts cause obvious performance decrement on video. *Annals of Biomedical Engineering, 48*(11), 2667–2677.

Brown, B. A., Daniel, R. W., Chancey, V. C., & Rooks, T. F. (2021). Parametric evaluation of head center of gravity acceleration error from rigid body kinematics assumptions used in environmental sensors. In *ASME International Mechanical Engineering Congress and Exposition* (Vol. 85598, pp. V005T05A074). American Society of Mechanical Engineers.

Camarillo, D. B., Shull, P. B., Mattson, J., Shultz, R., & Garza, D. (2013). An instrumented mouthguard for measuring linear and angular head impact kinematics in American football. *Annals of Biomedical Engineering*, *41*(9), 1939–1949.

DVBIC. (2020). *DOD Numbers for TBI 2000-2019 Q4*. DVBIC.

Gronwall, D., & Wrightson, P. (1975). Cumulative effect of concussion. *The Lancet*, *306*(7943), 995–997.

Guskiewicz, K. M., Marshall, S. W., Bailes, J., McCrea, M., Cantu, R. C., Randolph, C., & Jordan, B. D. (2005). Association between recurrent concussion and late-life cognitive impairment in retired professional football players. *Neurosurgery*, *57*(4), 719–726. https://doi.org/10.1227/01.NEU.0000175725.75780.DD

Jones, B., Tooby, J., Weaving, D., Till, K., Owen, C., Begonia, M., Stokes, K., Rowson, S., Phillips, G., Hendricks, S., & Tierney, G. (2022). Ready for impact? A validity and feasibility study of instrumented mouthguards (iMGs). *medRxiv.*

Kieffer, E. E., Begonia, M. T., Tyson, A. M., & Rowson, S. (2020). A two-phased approach to quantifying head impact sensor accuracy: In-laboratory and on-field assessments. *Annals of Biomedical Engineering*, *48*(11), 2613–2625.

Kuo, C., Wu, L. C., Hammoor, B. T., Luck, J. F., Cutcliffe, H. C., Lynall, R. C., & Camarillo, D. B. (2016). Effect of the mandible on mouthguard measurements of head kinematics. *Journal of Biomechanics*, *49*(9), 1845–1853.

Liu, Y., Domel, A. G., Yousefsani, S. A., Kondic, J., Grant, G., Zeineh, M., & Camarillo, D. B. (2020). Validation and comparison of instrumented mouthguards for measuring head kinematics and assessing brain deformation in football impacts. *Annals of Biomedical Engineering, 48*(11), 2580–2598.

Martin, P. G., Hall, G. W., Crandall, J. R., & Pilkey, W. D. (1998). Measuring the acceleration of a rigid body. *Shock and Vibration*, *5*(4), 211–224.

McAllister, T., & McCrea, M. (2017). Long-term cognitive and neuropsychiatric consequences of repetitive concussion and head-impact exposure. *Journal of Athletic Training*, *52*(3), 309–317.

McCrea, M., Hammeke, T., Olsen, G., Leo, P., & Guskiewicz, K. (2004). Unreported concussion in high school football players: Implications for prevention. *Clinical Journal of Sport Medicine*, *14*(1), 13–17.

O'Neil, M. E., Carlson, K., Storzbach, D., Brenner, L., Freeman, M., Quiñones, A., Motu'apuaka, M., Ensley, M., & Kansagara, D. (2013). *Complications of mild traumatic brain injury in veterans and military personnel: A systematic review*. Department of Veterans Affairs.

Society of Automotive Engineers (SAE). (1995). Instrumentation for impact test—Part 1: Electronic instrumentation. *SAE Handbook* (pp. 384-392). SAE.

Siegmund, G. P., Guskiewicz, K. M., Marshall, S. W., DeMarco, A. L., & Bonin, S. J. (2016). Laboratory validation of two wearable sensor systems for measuring head impact severity in football players. *Annals of Biomedical Engineering*, *44*(4), 1257–1274.

Siegmund, G. P., Guskiewicz, K. M., Marshall, S. W., DeMarco, A. L., & Bonin, S. J. (2014). A headform for testing helmet and mouthguard sensors that measure head impact severity in football players. *Annals of Biomedical Engineering*, *42*(9), 1834–1845.

Walilko, T. J., Viano, D. C., & Bir, C. A. (2005). Biomechanics of the head for Olympic boxer punches to the face. *British Journal of Sports Medicine*, *39*(10), 710–719.

Appendix A. Test Matrices for Indirect and Direct Impact Conditions

Table A1. Indirect Impact Matrix using IMM

Headform	Sensor number	Impact energy level (J)	Number of tests
MLSH	1	130	3
		198	3
		266	3
		334	3
	2	130	3
		198	3
		266	3
		334	3
	3	130	3
		198	3
		266	3
		334	3
NOCSAE	1	130	3
		198	3
		266	3
		334	3
	2	130	3
		198	3
		266	3
		334	3
	3	130	3
		198	3
		266	3
		334	3
Total number of tests:			72

Table A2. Direct Impact Matrix using IMM

Headform	Sensor number	Head CG energy level	Headgear	Number of tests
MLSH	4	Flyweight	No	3
		Super heavyweight	No	3
		Flyweight	Yes	3
		Super heavyweight	Yes	3
	5	Flyweight	No	3
		Super heavyweight	No	3
		Flyweight	Yes	3
		Super heavyweight	Yes	3
	6	Flyweight	No	3
		Super heavyweight	No	3
		Flyweight	Yes	3
		Super heavyweight	Yes	3
NOCSAE	4	Flyweight	No	3
		Super heavyweight	No	3
		Flyweight	Yes	3
		Super heavyweight	Yes	3
	5	Flyweight	No	3
		Super heavyweight	No	3
		Flyweight	Yes	3
		Super heavyweight	Yes	3
	6	Flyweight	No	3
		Super heavyweight	No	3
		Flyweight	Yes	3
		Super heavyweight	Yes	3
Total number of tests:				72

Appendix B. Direct Impact Test Energy Conditions

Table B1. Super Heavyweight Energies Transferred to Headforms

	MLSH (J)	NOCSAE (J)	Walilko (J)
	28.2	21.5	20
	29.6	21.2	28
	29.2	20.6	32
	29.9	21.3	31
	29.4	19.8	32
	29.8	19.7	-
	30.2	23.7	-
	29.9	22.6	-
	30.3	23.4	-
Mean	**29.6**	**21.5**	**28.6**
SD	**0.64**	**1.46**	**5.08**
Maximum	**30.3**	**23.7**	**32**
Minimum	**28.2**	**19.7**	**20**

Note. Estimated energies transferred to the head from the pendulum under direct impacts calculated for the MLSH and NOCSAE tests with headgear. Energies from Walilko et al. (2005) were used to ensure the minisled and pendulum were successful at producing the desired energy range. Energies are for a Super Heavyweight. *SD is the standard deviation.

Table B1. Flyweight Energies Transferred to Headforms

	MLSH (J)	NOCSAE (J)	Walilko (J)
	17.4	14.6	17
	18.4	13.5	14
	18.9	13.2	20
	17.3	13.4	9
	19.3	12.6	20
	18.6	12.3	13
	18.0	14.2	14
	17.9	14.5	-
	18.4	15.8	-
Mean	**18.3**	**13.8**	**15.3**
SD	**0.66**	**1.09**	**3.99**
Maximum	**19.3**	**15.8**	**20**
Minimum	**17.3**	**12.3**	**9**

Note. Estimated energies transferred to the head from the pendulum under direct impacts calculated for the MLSH and NOCSAE tests with headgear. Energies from Walilko et al. (2005) were used to ensure the minisled and pendulum were successful at producing the desired energy range. Energies are for a Flyweight. *SD is the standard deviation.

Appendix C. Supplemental Figures

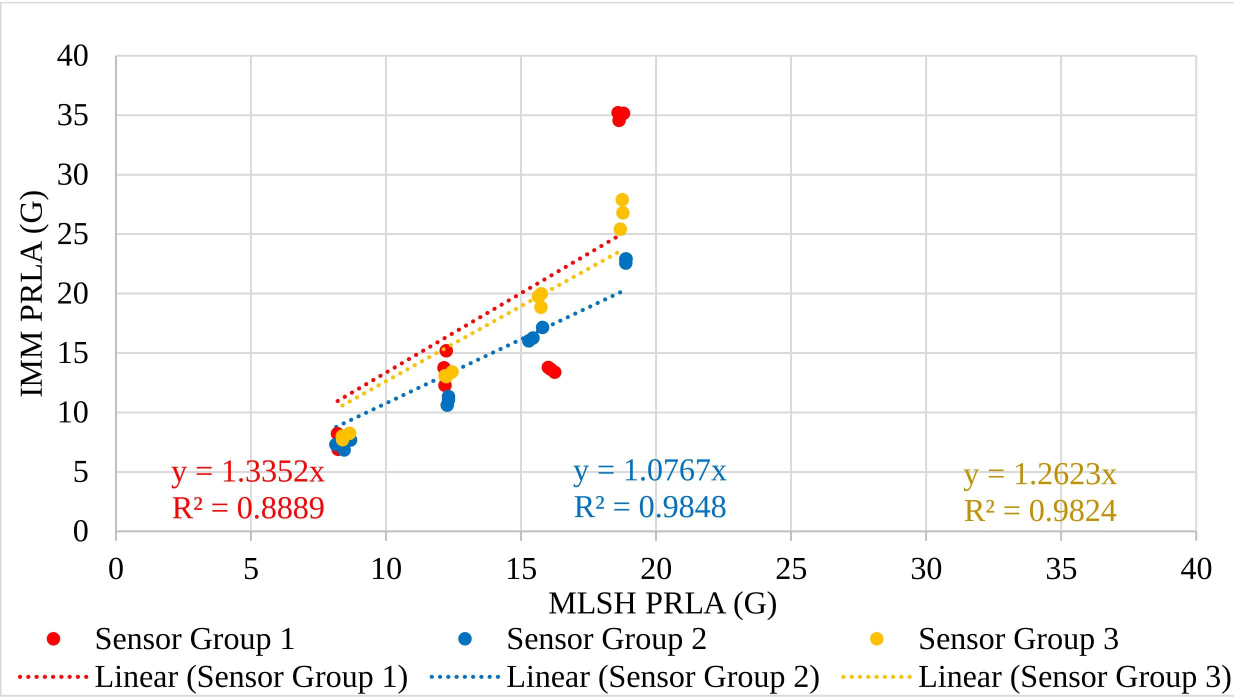

(a)

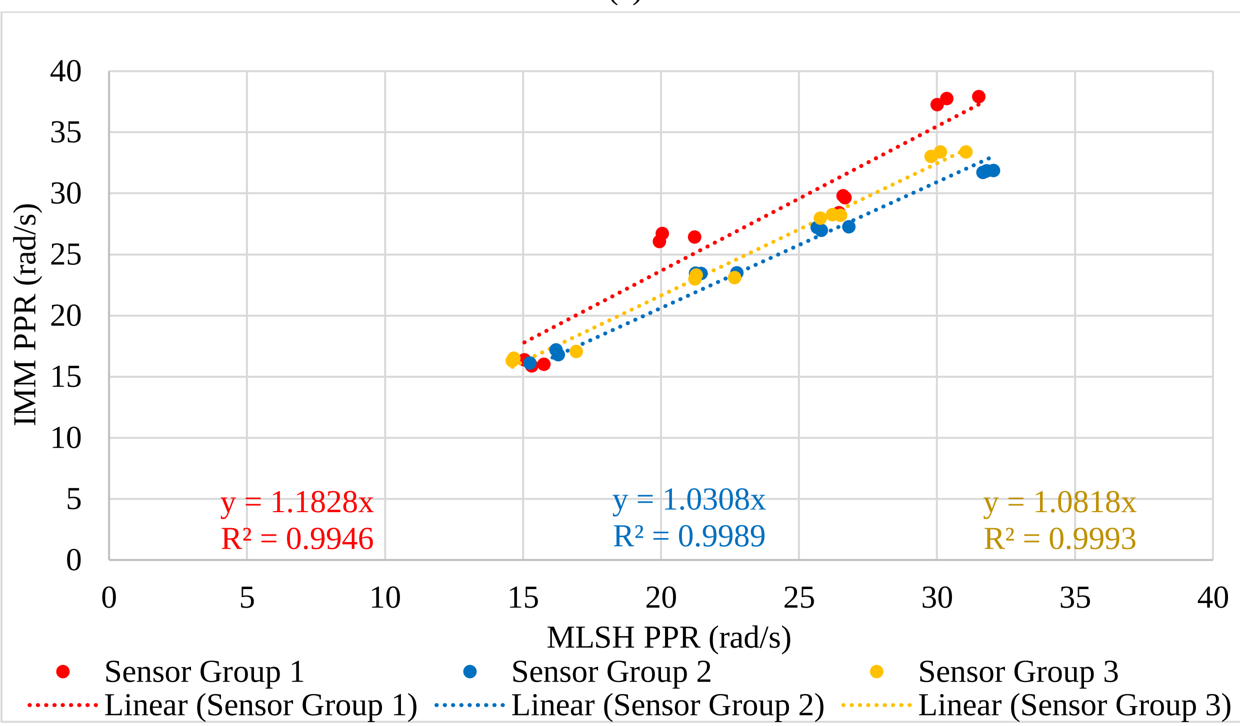

(b)

Figure C1. Scatter plots of instrumented mouthguard versus MLSH peak kinematics broken down by sensor group for (a) linear acceleration and (b) angular velocity during indirect impacts.

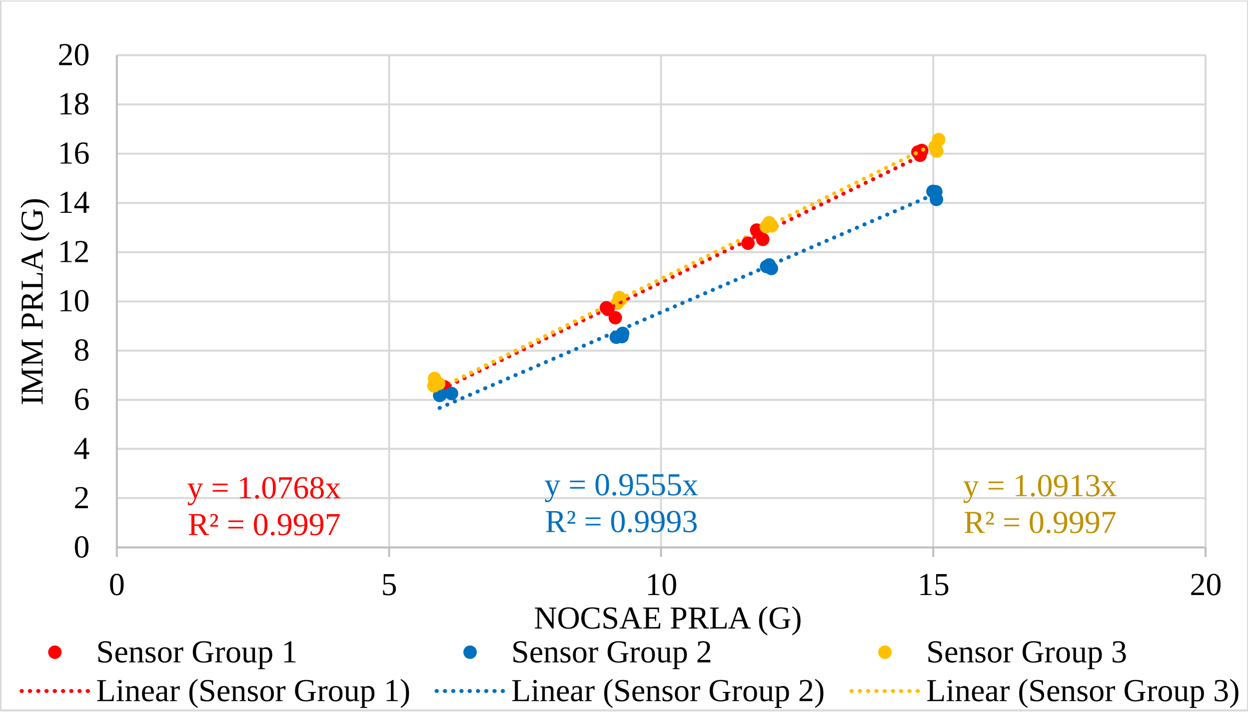

(a)

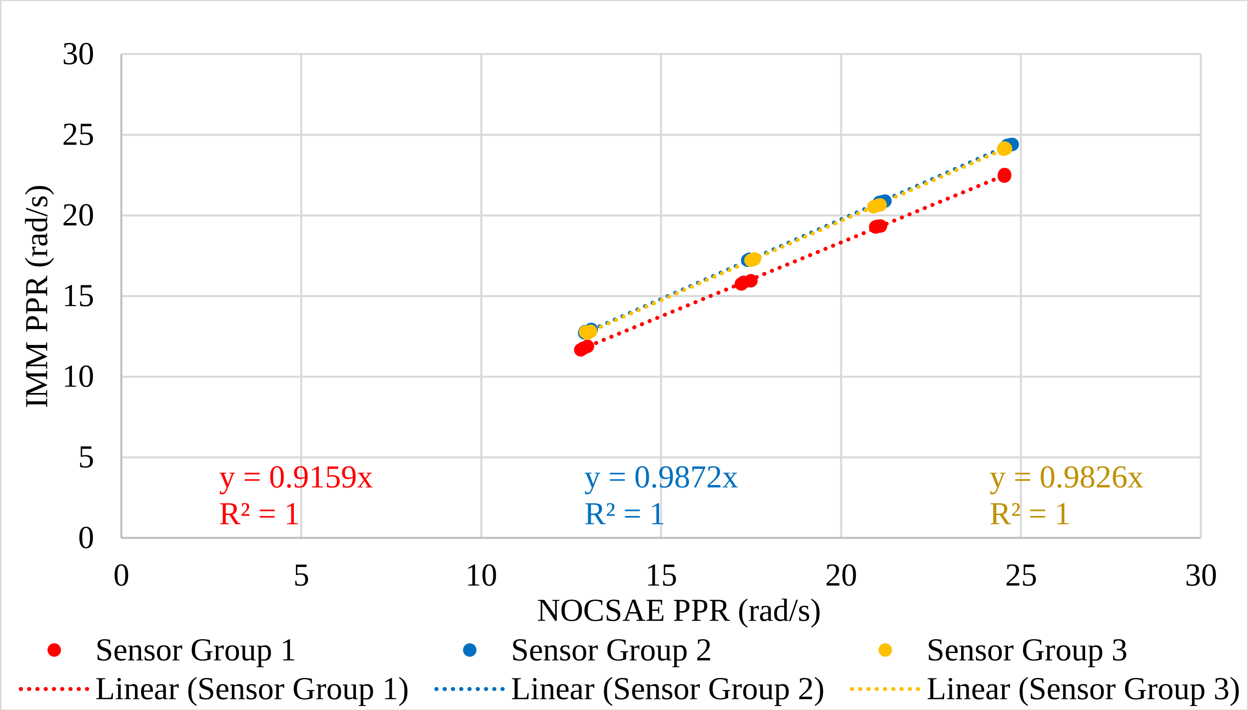

(b)

Figure C2. Scatter plots of IMM versus NOCSAE peak kinematics broken down by sensor group for (a) linear acceleration and (b) angular velocity during indirect impacts.

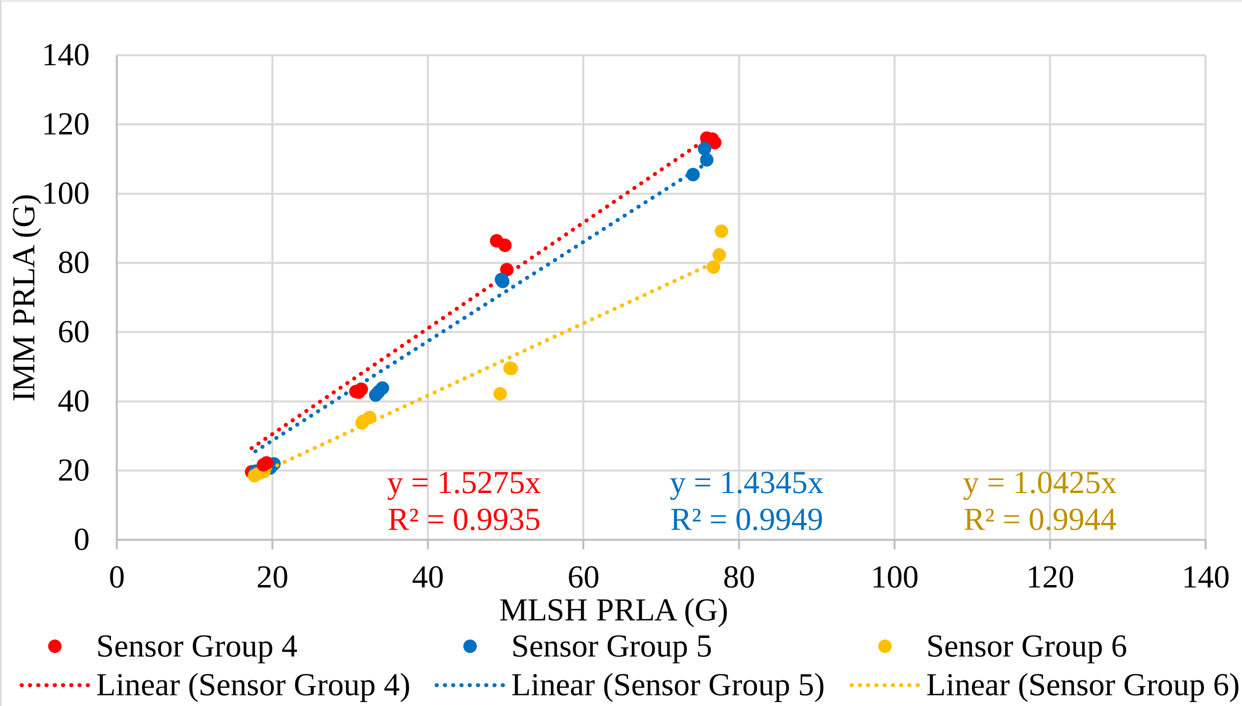

(a)

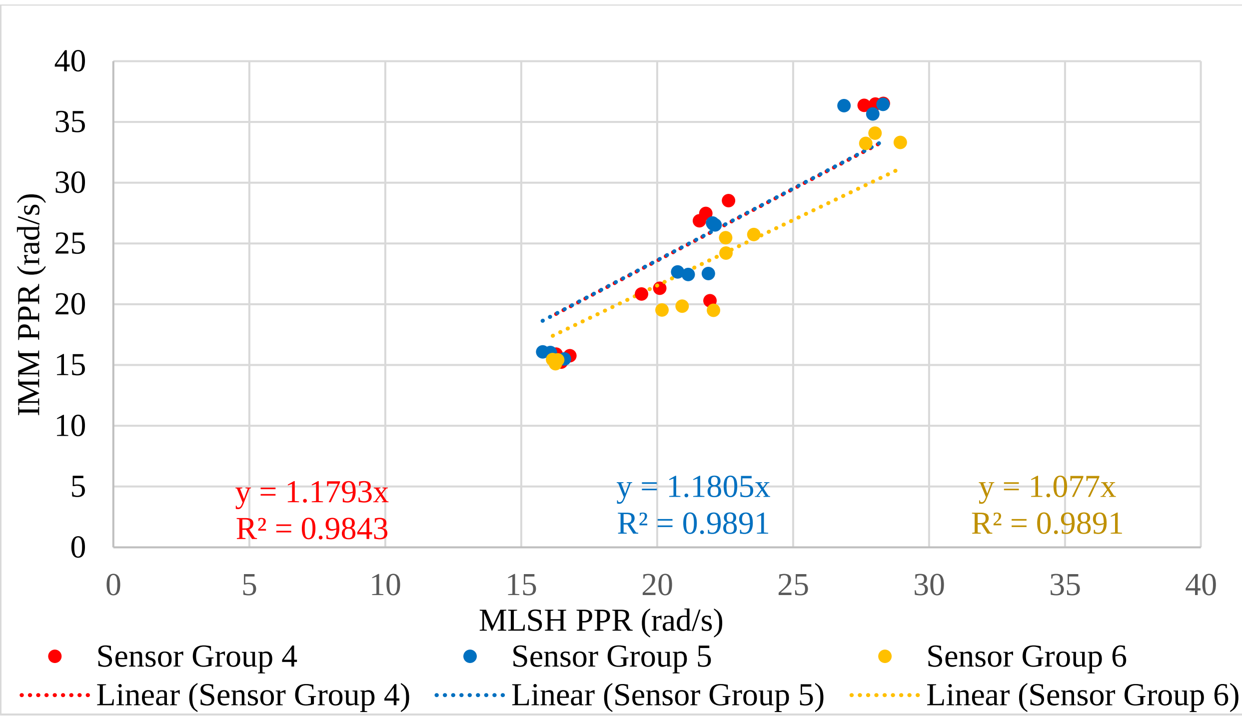

(b)

Figure C3. Scatter plots of IMM versus MLSH peak kinematics broken down by sensor group for (a) linear acceleration and (b) angular velocity during direct impacts.

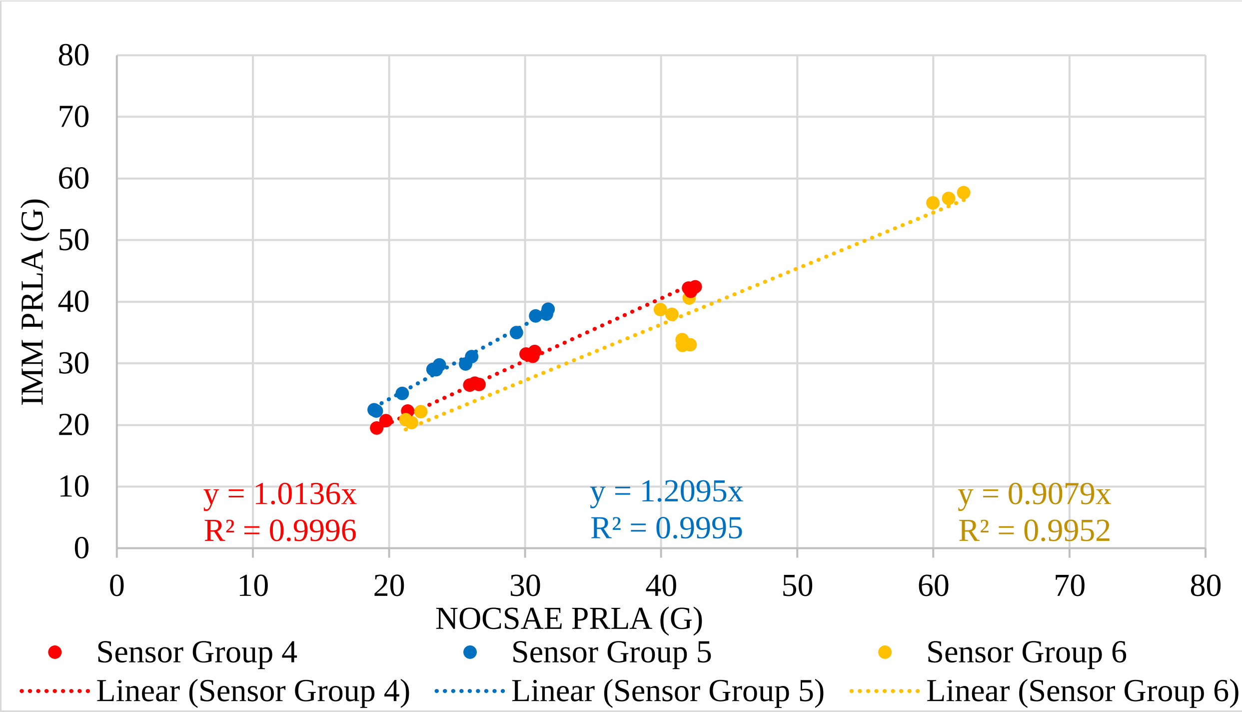

(a)

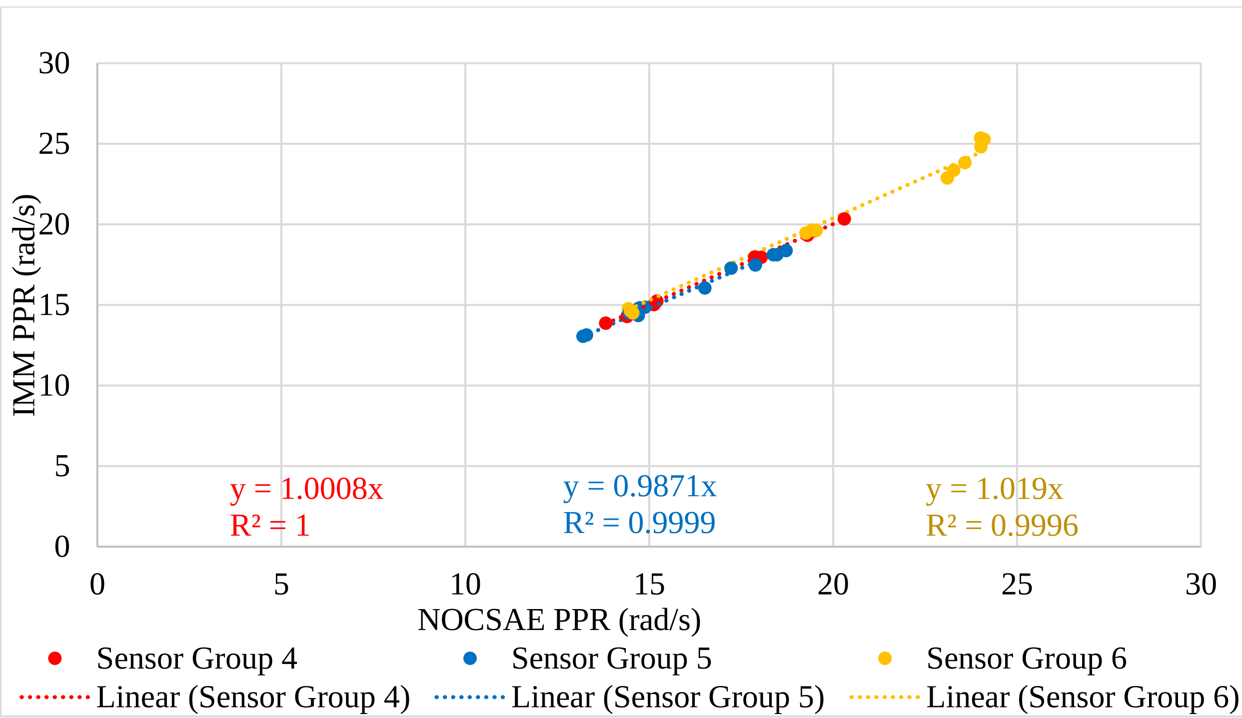

(b)

Figure C4. Scatter plots of IMM versus NOCSAE peak kinematics broken down by sensor group for (a) linear acceleration and (b) angular velocity during direct impacts.

U.S. ARMY AEROMEDICAL RESEARCH LABORATORY

FORT NOVOSEL, ALABAMA

Optimizing

HUMAN PROTECTION
AND PERFORMANCE

since 1962

All of USAARL's science and technical informational documents are available for download from the Defense Technical Information Center.
https://discover.dtic.mil/results/?q=USAARL

U.S. ARMY

FORGE THE FUTURE

FUTURES COMMAND

MRDC